Ionization of one-dimensional alkali atoms by microwave fields

2001 J. Phys. A: Math. Gen. 34 8101

(http://iopscience.iop.org/0305-4470/34/39/310)

INSTITUTE OF PHYSICS PUBLISHING JOURNAL OF PHYSICS A: MATHEMATICAL AND GENERAL

J. Phys. A: Math. Gen. **34** (2001) 8101–8118 PII: S0305-4470(01)25347-5

Ionization of one-dimensional alkali atoms by microwave fields

D Campos[1], **M C Spinel and J Madroñero**

Departamento de Física, Universidad Nacional, Bogotá, Colombia

E-mail: dcamposr@ciencias.unal.edu.co

Received 25 May 2001
Published 21 September 2001
Online at stacks.iop.org/JPhysA/34/8101

Abstract

We consider the classical dynamics of alkali atoms in microwave fields. The atom is described by a simplified one-dimensional integrable model that includes two atom-dependent parameters, σ and C. Chirikov's overlap criterion is applied for determining the conditions needed to produce chaotic motion (ionization) when the atom is placed in a periodically varying electric field. In order to test the ionization conditions we analyse the behaviour of single classical trajectories for several values of the field strength by numerically integrating the Hamilton's equations. The results validate Chirikov's predictions for low resonances and show that the ionization process depends on the field's phase γ. However, by changing γ we can get physically equivalent trajectories if we also choose the right initial conditions for the Hamilton equations. The dynamical process along a classical trajectory is characterized by suitable quantities and some crucial properties are exploited for *predicting ionization* far before the ionization time is reached.

PACS numbers: 05.45.+b, 95.10.Fh, 11.10.Ef, 32.80.Rm

1. Introduction

Ionization of highly excited hydrogen atoms by microwave photons is one of the first experiments in atomic physics associated to quantum chaos ([1] and references therein). Leopold and Percival [2] were the first ones to apply a classical theory and obtain excellent agreement with the enhanced 'ionization' rates reported by the Bayfield–Koch experiment [3]. Since then there have been many further experiments and calculations (for a recent review see [4], and for the theoretical background [5–8]).

Similarly, during the last decades a considerable set of experimental data has been accumulated in experiments on Rydberg states of alkali atoms exposed to microwave

[1] Address for correspondence: Apartado Aéreo 103698, Bogotá, Colombia.

Table 1. Values of the parameters σ and C for the alkali atoms [16].

Atom	$Z-\sigma$	C
Li	1.211	1.78
Na	1.846	6.00
K	1.846	7.41
Rb	1.846	7.76
Cs	1.846	8.49

fields [9–14]. These systems, that straddle the classical-quantal border, are ideal candidates for studying the behaviour of quantal systems which show nonlinear dynamics in their classical limit [14, 15].

In this paper we present an one-dimensional model to describe the classical dynamics of highly excited alkali atoms moving through a microwave cavity. Notwithstanding that the proposed model is a simple approximation of the real physical system, it can provide useful insights for theoretical studies of the quantum-classical correspondence in the vast area of quantum chaos.

The model has its roots in an example treated by Eder [16]. In his book on Quantum Mechanics, he assumes that the multi-electron *three-dimensional* alkali atom can be described by considering only the outer-valency-electron motion in a spherical symmetric field generated by the nucleus (charge Ze) and the inner electrons. Since the core is spherically symmetric, the valence electron moves in an effective central potential $V_0(r) = -(Z-\sigma)e^2/r + C\hbar^2/(2\mu r^2)$, where $-e$, μ, and r are charge, reduced mass, and distance electron–nucleus, respectively. The repulsive contribution $C\hbar^2/(2\mu r^2)$ is meant to mimic the influence of the Pauli exclusion effect and the charge repulsion between the valence electron and the electrons of the core. It is adopted because such a potential leads to an analytically solvable eigenvalue problem, but not because its general form is founded on any theoretical basis.

With this choice of $V_0(r)$ the analytical solution of the radial Schrödinger equation provides the following energy levels:

$$E_{n_0\,\ell} = -\frac{1}{2}\left[\frac{Z-\sigma}{n_0 + f(\ell)}\right]^2 \frac{\mu}{m_e}\varepsilon_0$$

where $\ell = 0, 1, 2, \ldots$ is the angular momentum, $n_0 = 1, 2, 3, \ldots$ the principal quantum number, m_e the electron's mass, $\varepsilon_0 = m_e e^4/\hbar^2$ the atomic energy unit and $f(\ell) = \left[(\ell + 1/2)^2 + C\right]^{1/2} - (\ell + \frac{1}{2})$. The model involves a phenomenological potential $V_0(r)$ depending on two parameters (σ and C) that are determined by comparison of $E_{n_0\,\ell}$ with the alkali spectra [16]. Table 1 shows the values obtained by Eder [16] for lithium, sodium, potassium, rubidium and caesium.

As in the microwave-ionization hydrogen problem [6, 17–19] we now introduce a *one-dimensional* model for describing an alkali atom in a microwave field. Let us assume that for a high-quantum principal number n_0 and angular momentum $\ell = 0$ the unperturbed alkali atom can be described by the one-dimensional Hamiltonian

$$H_0(z, p) = \frac{p^2}{2\mu} - \frac{(Z-\sigma)e^2}{z} + \frac{C\hbar^2}{2\mu}\frac{1}{z^2} = -E_0 \qquad E_0 > 0 \tag{1}$$

where z ($z \geqslant 0$), p and $-E_0$ are position, momentum and total energy of the valence electron respectively. $V_0(z)$ has a minimum value $-\mu(Z-\sigma)^2 e^4/(2C\hbar^2)$ at equilibrium distance $C\hbar^2/(\mu(Z-\sigma)e^2)$, and becomes positive for distances $0 < z < C\hbar^2/(2\mu(Z-\sigma)e^2)$. For the values $\sigma = 0$ and $C = 0$, $V_0(z)$ reproduces the potential energy of the one-dimensional hydrogen atom.

The alkali atom in a linearly z-polarized microwave field is then described by the Hamiltonian

$$H(z, p, t) = \frac{p^2}{2\mu} - \frac{(Z-\sigma)e^2}{z} + \frac{C\hbar^2}{2\mu}\frac{1}{z^2} - e\mathcal{F}z\sin(\omega t + \gamma) = H_0 + V(t) \qquad e > 0 \qquad (2)$$

where $V(t) = -e\mathcal{F}z\sin(\omega t + \gamma)$ is the interaction energy between the electron and the microwave field characterized by angular frequency ω and amplitude $\mathcal{F}$. Here γ is a free parameter that gives the phase of the field.

The Hamiltonian (2) offers a simple one-dimensional model system for testing classical chaos features. The electron, initially bounded by the potential $V_0(z)$, undergoes a transition to chaos under the influence of a periodic external electric perturbation $V(t)$. However, it is worth noting that the model (2) has a set of limitations. For example, it does not consider the angular motion of the Rydberg electron and the anisotropy of the core with non-zero angular momentum. The presence of core anisotropy can produce quadrupole moment and tensor polarizability interactions which cause energy levels to split. The spin of the active electron is also ignored, but it could be justified considering that the core's electrons and the high-n_0 active electron are confined to well separated regions of space, which eliminates short-range interactions such as exchange and partial screening of the nuclear charge.

In this paper we study the classical dynamics of ionization phenomenon. We first solve Hamilton equations derived from the unperturbed Hamiltonian (1) using action-angle variables (section 2). We then consider the alkali atom in the presence of the microwave field and apply Chirikov's criterion [20–22] to determine the critical electric-field strengths at which ionization (chaos) will occur (section 3). In section 4 we numerically solve Hamilton equations obtained from the full Hamiltonian (2). We validate Chirikov's criterion and characterize the dynamics of the ionization process by introducing suitable quantities, including the electron energy change due to the perturbation $V(t)$. We also exploit some crucial properties for predicting ionization far before the ionization time is reached. In section 5 we present some conclusions.

2. Dynamics of the unperturbed system

We consider the unperturbed alkali atom described by the Hamiltonian (1) and seek a canonical transformation connecting position and momentum (z, p) with action-angle variables (θ, I).

The valence electron with energy $-E_0$ has turning points z_0 and z_1 ($z_0 < z_1$) given by

$$z_0 = \frac{a}{b + \sqrt{b^2 - a}} \qquad z_1 = \frac{a}{b - \sqrt{b^2 - a}} \qquad (3)$$

with

$$a := \frac{C\hbar^2}{2\mu E_0} = z_0 z_1 \qquad b := \frac{(Z-\sigma)e^2}{2E_0} = \frac{1}{2}(z_0 + z_1). \qquad (4)$$

The momentum p of the electron can be written as

$$p(z) = \pm\frac{(2\mu E_0(z - z_0)(z_1 - z))^{1/2}}{z} \qquad (5)$$

where, by *convention*, the upper sign stands for motion from z_0 to z_1 with $p(z) \geqslant 0$, and the lower sign for motion from z_1 to z_0 with $p(z) \leqslant 0$. The momentum $|p(z)|$ exhibits a maximum at distance $z_m = 2z_0z_1/(z_0 + z_1)$.

In the case of one-dimensional hydrogenic atoms ($C = 0, \sigma = 0$), the electron reverses its momentum abruptly at $z = 0$. Therefore, we must set $z_0 = 0$ and $z_1 = 2b$ which simplifies (5) to $p(z) = \pm(2\mu E_0(z_1 - z)/z)^{1/2}$. The momentum $|p(z)|$ becomes infinity at the origin, $z_m = 0$.

In terms of the canonical-action variable

$$I = \frac{1}{2\pi}\oint p\,\mathrm{d}z = \frac{1}{2\pi}\left\{\int_{z_0}^{z_1} p_+\,\mathrm{d}z + \int_{z_1}^{z_0} p_-\,\mathrm{d}z\right\} = (\mu E_0/2)^{1/2}\left(\sqrt{z_1}-\sqrt{z_0}\right)^2$$

the unperturbed Hamiltonian (1) becomes

$$H_0(I) = -E_0 = -\frac{\mu}{2}\left(\frac{(Z-\sigma)e^2}{I+I_*}\right)^2 \tag{6}$$

with $I_* = \hbar C^{1/2}$. Note that equation (6) reproduces the quantum spectrum of alkali atoms (see introduction) if we set $(I+I_*)/\hbar = n_0 + \left((\ell+1/2)^2 + C\right)^{1/2} - (\ell+1/2)$, where n_0 and $\ell = 0$ are the principal and angular-momentum quantum numbers. In comparison with the hydrogenic case ($C = 0$, $I = n_0\hbar$), the non-vanishing parameter $C > 0$ in the alkali atoms yields a shift in the linear relation between action I and principal quantum number n_0, namely $I = (n_0 - N_C)\hbar$, where $N_C := (1/2+C^{1/2}) - (1/4+C)^{1/2} > 0$ is an atom-dependent constant (see table 1). The parameter N_C increases from $N_0 = 0$ to $N_\infty = 1/2$.

From the Hamilton equation $\mathrm{d}\theta/\mathrm{d}t = \partial H_0(I)/\partial I$, the solution for the angle variable can be expressed as

$$\theta(t) = \theta_\mathrm{i} + \Omega(I)(t - t_\mathrm{i}) \tag{7}$$

where $\Omega(I) := \partial H_0/\partial I$ defines the nonlinear characteristic frequency of the system

$$\Omega(I) = \frac{\mu}{(Z-\sigma)e^2}\left(\frac{(Z-\sigma)e^2}{I+I_*}\right)^3 = \frac{2(2E_0/\mu)^{1/2}}{z_0+z_1}. \tag{8}$$

In (7) $\theta_\mathrm{i} = \theta(t_\mathrm{i})$ is an integration constant. We set $z(t_0) = z_0$ and $\theta_0 = \theta(t_0)$ for motion from z_0 to z_1, and $z(t_1) = z_1$ and $\theta_1 = \theta(t_1)$ for motion from z_1 to z_0.

Now, the Hamilton equation $\mu\,\mathrm{d}z/\mathrm{d}t = p$ implies

$$\frac{z\,\mathrm{d}z}{\sqrt{(z-z_0)(z_1-z)}} = \pm\left(\frac{2E_0}{\mu}\right)^{1/2}\mathrm{d}t.$$

Integration of this equation yields

$$t - t_\mathrm{i} = \left(\frac{\mu}{2E_0}\right)^{1/2}\left\{\mp\frac{1}{2}(z_1-z_0)\sin\varphi + \frac{1}{2}(z_1+z_0)\varphi\right\} \qquad \varphi\in[0,\pi] \tag{9}$$

where φ is an auxiliary variable defined by

$$\varphi = \arccos\left\{\pm\frac{z_1+z_0-2z}{z_1-z_0}\right\} \qquad \varphi\in[0,\pi]. \tag{10}$$

By substituting (9) in (7) and using (8) we get

$$\theta = \theta_\mathrm{i} \pm c_0(I)\sin\varphi + \varphi \tag{11}$$

where we define

$$c_0(I) := \frac{z_1-z_0}{z_1+z_0} = \left[1 - \left(\frac{I_*}{I+I_*}\right)^2\right]^{1/2}. \tag{12}$$

For alkali atoms $z_0 \neq 0$ and $I_* \neq 0$, hence $0 \leqslant c_0(I) < 1$. For hydrogenic atoms $z_0 = 0$, $I_* = 0$ and $c_0(I) = 1$. Hereafter, in order to simplify the equations we will write c_0 instead of $c_0(I)$.

Equation (9) implies $t_1 = t_0 + (\mu/(2E_0))^{1/2}(z_1+z_0)\pi/2$. As a consequence, the characteristic period of the unperturbed motion is

$$T = \left(\frac{\mu}{2E_0}\right)^{1/2}(z_1+z_0)\pi. \tag{13}$$

From (11) we obtain $\theta_1 = \theta_0 + \pi$, that is, the angular variable θ has initial value θ_0 and period 2π. By using (10) and (11) we find the relation

$$z = \tfrac{1}{2}(z_1 + z_0)\,(1 \mp c_0 \cos\varphi) \qquad \varphi \in [0, \pi]. \tag{14}$$

Replacement of this equation in (5) yields

$$p = \pm(2\mu E_0)^{1/2} \frac{c_0 \sin\varphi}{1 \mp c_0 \cos\varphi} \qquad \varphi \in [0, \pi]. \tag{15}$$

Equations (14) and (15) specify the valence electron trajectory in terms of the parameter $\varphi \in [0, \pi]$. They also define, through (11) and (12), the canonical transformation $(z, p) \to (\theta, I)$ that provides the relation with θ and I variables. Note that (14) and (15) can be written as $z = \frac{1}{2}(z_1 + z_0)\,(1 - c_0 \cos\varphi)$ and $p = (2\mu E_0)^{1/2}(c_0 \sin\varphi)/(1 - c_0 \cos\varphi)$ for $\varphi \in [0, 2\pi]$.

3. Chirikov's condition for ionization

In this section we transform the full perturbed Hamiltonian (2) to action-angle variables (θ, I) and determine the analytical expression for the critical electric-field amplitude according to Chirikov's overlap criterion. We start by writing the interaction potential $V(t)$ as

$$V(t) = -b(I)e\mathcal{F}\,(1 - c_0 \cos\varphi)\sin(\omega t + \gamma) \qquad e > 0 \quad \varphi \in [0, 2\pi] \tag{16}$$

where, according to (4) and (6),

$$b(I) = \frac{1}{2}(z_0 + z_1) = \frac{(I + I_*)^2}{\mu(Z - \sigma)e^2}.$$

As we already quoted the angle variable θ has initial value θ_0 and period 2π. Since $\varphi = \varphi(\theta)$ and $\cos\varphi(\theta)$ are periodic functions of θ we can use the expansion [23]

$$\cos(\varphi(\theta)) = \sum_{n=-\infty}^{\infty} a_n \exp(\mathrm{i}n\theta) \tag{17}$$

with coefficients

$$a_n = \frac{1}{2\pi} \int_{\theta_0}^{\theta_0 + 2\pi} \cos(\varphi(\theta)) \exp(-\mathrm{i}n\theta)\,\mathrm{d}\theta.$$

We can separate the contributions of intervals $\theta_0 \leqslant \theta \leqslant \theta_1$ and $\theta_1 \leqslant \theta \leqslant \theta_0 + 2\pi$, apply (11) to change the integration variable from θ to φ, and use Bessel's integrals [24]

$$\begin{aligned} J_n(x) &= \frac{1}{\pi} \int_0^{\pi} \cos(n\varphi - x\sin\varphi)\,\mathrm{d}\varphi \\ &= \frac{x}{n\pi} \int_0^{\pi} \cos\varphi \cos(n\varphi - x\sin\varphi)\,\mathrm{d}\varphi \qquad n \text{ integral} \end{aligned} \tag{18}$$

to obtain

$$a_n = \exp(-\mathrm{i}n\theta_0)\frac{1}{n} J_n'(nc_o) \tag{19}$$

where $J_n'(x)$ is the x-derivative of the integral Bessel function (18).

From (17) and (19) equation (16) yields

$$V(t) = -b(I)e\mathcal{F} \sum_{n=-\infty}^{\infty} \{A(n, c_o) - \delta_{n0}\} \exp\{-\mathrm{i}n(\theta - \theta_0)\} \sin(\omega t + \gamma) \tag{20}$$

where δ_{n0} is the Kronecker delta and the coefficients $A(n, c_0)$ are defined by

$$A(n, c_0) = \frac{c_0(I)}{n} J_n'(nc_0(I)). \tag{21}$$

It follows from (21) and by differentiation of (18) that $A(n, c_0) = A(-n, c_0)$. Thus, we can write the full time-dependent Hamiltonian (2) in terms of the unperturbed action-angle variables as follows:

$$H(\theta, I, t) = H_0(I) - b(I)e\mathcal{F} \sum_{n=-\infty}^{\infty} \{A(n, c_o) - \delta_{n0}\} \sin\{n(\theta - \theta_0) - (\omega t + \gamma)\}. \tag{22}$$

This yields an infinite superposition of rotating sine potentials indexed by the integer n.

An interesting remark concerning the coefficient $A(n, c_0)$ is adequate at this point. We recall the integral representation [25]

$$J_n'(N) = \frac{1}{2\pi \mathrm{i}} \int_{\infty-\pi\mathrm{i}}^{\infty+\pi\mathrm{i}} F(u, \alpha) \exp(NF(u, \alpha))\, \mathrm{d}u$$

where the parameter c_0 is written as $c_0 = \operatorname{sech}\alpha$, with $\alpha \geqslant 0$, $N := nc_0 = n \operatorname{sech}\alpha$ and $F(u, \alpha) := \sinh u - u\cosh\alpha$. The values $u_\pm(\alpha) = \pm\alpha$ are saddle-points at which $\partial F/\partial u$ vanishes. They coalesce as $c_0 \to 1$. Then, if $n \to \infty$ and $0 < c_0 < 1$ the main contribution comes from the two saddle-points $\pm\alpha$. When $c_0 = 1$ only the stationary point $\alpha = 0$ contributes. Applying the method of asymptotic expansion as described in [26], we could derive an asymptotic expansion of $J_n'(nc_0)$ which would be uniformly valid in a neighbourhood around the exceptional value of c_0. This might allow us to simultaneously study alkali and hydrogenic atoms.

Let us now consider *Chirikov's overlap criterion* for determining the critical electric-field values that allows ionization through resonance overlaps. This criterion postulates that 'the last KAM surface between two lowest-order resonances is destroyed when the sum of half-widths of the two island separatrices formed by the resonances, but calculated independently of one another, just equals the distance between resonances' [22]. To apply this criterion, we first determine the position and separation of resonances recalling first-order perturbation theory and consider the dynamics in the neighbourhood of a primary resonance to determine its width.

When the interaction potential $V(t)$ is a perturbation for the system described by H_0, the solution of Hamilton equations derived from (22) is sought in the form [22] $I = I^{(0)} + \varepsilon I^{(1)} + \cdots$ and $\theta = \theta^{(0)} + \varepsilon\theta^{(1)} + \cdots$. The solution of the unperturbed system studied in section 2 yields the zero-order approximation. That is, $I^{(0)} = I =$ constant and $\theta^{(0)} = \theta(t) = \Omega(I)(t - t_0) + \theta_i$. The singularities obtained from first-order approximation $(\theta^{(1)}, I^{(1)})$ define the resonance condition $n\Omega(I) - \omega = 0$.

From this and (8) we find that resonances occur for the set of actions

$$I_n = \left\{\frac{n\mu}{\omega}(Z - \sigma)^2 e^4\right\}^{1/3} - I_* \qquad n = \pm 1, \pm 2, \pm 3, \ldots. \tag{23}$$

So, the separation between two consecutive resonant actions is

$$\delta_n := I_{n+1} - I_n = \left[\frac{\mu}{\omega}(Z - \sigma)^2 e^4\right]^{1/3} \left[(n+1)^{1/3} - n^{1/3}\right]. \tag{24}$$

We observe that separation between resonant actions decreases as n growths and becomes $\delta_n \approx (I_n + I_*)/(3n)$ for large n. Equation (24) indicates that for a fixed value of ω the distance δ_n increases with the value of the effective charge $(Z - \sigma)e$ of the core (alkali atoms) or of the atomic nucleus (hydrogen-like atoms, $\sigma = 0$).

Given one resonant action, from (6) and (23) we obtain the corresponding absolute values of the unperturbed energies

$$E_{0,n} = \frac{\mu}{2}\left[\frac{\omega}{n\mu}(Z - \sigma)e^2\right]^{2/3}. \tag{25}$$

Following the main idea used to analyse resonances [20], in phase-space regions where the action variable I is very close to the resonant action I_n the perturbation effect is dominated

by the corresponding term in expansion (22). In other words, in the neighbourhood of one particular n-primary resonance the dynamics behaviour of the system is governed by the Hamiltonian

$$H(\theta, I, t) = H_0(I) - b(I)e\mathcal{F}A(n, c_0)\sin\{n(\theta - \theta_0) - (\omega t + \gamma)\}. \tag{26}$$

Restricted to the neighbourhood of each primary-resonance we can define the canonical transformation $(\theta, I) \to (\Psi, \Delta I)$ with $\Delta I := I - I_n$ and $\Psi = \theta - \theta_0 - (\omega t + \gamma)/n$. Expanding the image of Hamiltonian (26) in a ΔI series up to second order for H_0 and first order for the interaction term, we obtain the following approximation:

$$\tilde{H} = -\frac{(\Delta I)^2}{2M} - U_0 \sin(n\Psi) \tag{27}$$

with

$$U_0(I_n) = b(I_n)e\mathcal{F}A(n, c_0(I_n)) \qquad \frac{1}{M} = 3\mu\frac{(Z-\sigma)^2e^4}{(I_n + I_*)^4} = 3\frac{\Omega(I_n)}{I_n + I_*}.$$

Here $\Omega(I_n)$ is the nonlinear characteristic frequency of the system defined by (8). Since (27) is similar to the Hamiltonian of the nonlinear pendulum [7,20] with small frequency oscillations $\tilde{\omega}_0^2 := U_0(I_n)/M$, it gives the pendulum approximation for alkali atoms.

From (27), the pendulum resonance width in I, given by the width of the trapping (libration) region of the pendulum [21], is

$$W_n = 4\left(|M|U_0(I_n)\right)^{1/2} = 4(I_n + I_*)^3\left[\frac{e\mathcal{F}A(n, c_0)}{3\mu^2[(Z-\sigma)e^2]^3}\right]^{1/2}. \tag{28}$$

According to Chirikov's criterion [20, 22], all KAM surfaces between n and $(n + 1)$ resonances are destroyed when $(W_{n+1} + W_n)/2 = g\,\delta_n$, where $g = 1$ when only overlaps between primary resonances are considered. In some systems, such as H-atom ionization by circularly polarized microwave fields [27,28], the presence of higher-order resonances is taken into account heuristically by the two-thirds rule, $g = 2/3$.

From the above condition and equations (28) and (24) we obtain the following expression for the *critical values of the electric field*:

$$\mathcal{F}_n^{\rm cr} = g^2\,\frac{3\left[\omega^4\mu^2(Z-\sigma)e^2\right]^{1/3}}{4e}\left\{\frac{(n+1)^{1/3} - n^{1/3}}{(n+1)\left[A(n+1, c_0)\right]^{1/2} + n\left[A(n, c_0)\right]^{1/2}}\right\}^2. \tag{29}$$

From (6) and (25) it is seen that the required unperturbed energy $H_0(I_n) = -E_{0,n}$ to prepare the valence electron in the n-primary resonance increases with n. So, one expects that the strength of the critical electric field required to ionize an alkali atom decreases with n. This is corroborated by (29) as illustrated in table 2. Therefore, according to Chirikov's criterion, if we prepare the valence electron with a given initial energy $-E_{0,n}$ and apply a microwave field $\mathcal{F} \geqslant \mathcal{F}_n^{\rm cr}$, the electron can reach the next resonance zone in phase space. Since the field amplitude is larger than that required for the overlapping of higher resonance zones, all KAM surfaces are destroyed and the electrons gradually can reach higher resonance regions, hence ionization induced by chaos should occur.

On the other hand (see text after equation (6)), from the relation $I_n = (n_0 - N_C)\hbar$ we can estimate the principal quantum number n_0 corresponding to the resonant energy $-E_{0,n}$. It is given as the integer part of (with $\ell = 0$)

$$n_0 = \frac{(Z-\sigma)e^2}{\hbar\sqrt{-2E_{0,n}/\mu}} - \left(\frac{1}{4} + C\right)^{1/2} + \frac{1}{2}. \tag{30}$$

Some particular values of n_0 for lithium are listed in table 3.

Table 2. Critical electric-field amplitude for the first seven resonances, with $\omega = 1.509 \times 10^{-6}$ au, and g a parameter (see text after equation (28)).

$\mathcal{F}_n^{\rm cr}/g^2$ ($\times 10^{-10}$ au)	$n=1$	$n=2$	$n=3$	$n=4$	$n=5$	$n=6$	$n=7$
Lithium	6.085 57	2.353 81	1.294 14	0.834 20	0.589 38	0.442 10	0.345 93
Sodium	7.003 75	2.708 95	1.489 40	0.960 06	0.678 30	0.508 81	0.398 12

Table 3. Approximated principal quantum number n_0 corresponding to the resonant energy $E_{0,n}$ for lithium.

Resonance	$n=1$	$n=2$	$n=3$	$n=4$	$n=10$	$n=20$	$n=30$
$-E_{0,n}$ ($\times 10^{-7}$ au)	747.353	470.803	359.29	296.587	161.012	101.431	77.4066
n_0	98	123	141	156	212	267	306

4. Dynamics of the classical-ionization process

In this section we study the system's dynamics for several primary resonances ($n = 1, 2, 3, 4$) and different values of the electric amplitude $\mathcal{F}$. To do this, we compare Chirikov's values of the electric field (29) with the numerical results for the classical onset of chaotic motion, which are obtained by scanning $\mathcal{F}$ and numerically solving the Hamilton equations derived from the full Hamiltonian (2).

For a suitable value of $\mathcal{F}$ the electron's classical trajectory is chaotic and, therefore, there is ionization for a sufficiently large finite time, $t_{\rm I}$. We introduce basic quantities to characterize the ionization process and propose a method for predicting ionization far before the ionization time $t_{\rm I}$ is reached. We also explore the role of the microwave field's phase γ in this process and introduce the concept of physically equivalent trajectories.

The starting point is given by the Hamilton equations derived from the full Hamiltonian (2), which describe the evolution of the valence electron in the microwave field:

$$\frac{{\rm d}z}{{\rm d}t} = \frac{p}{\mu} \qquad \frac{{\rm d}p}{{\rm d}t} = -(Z-\sigma)e^2\frac{1}{z^2} + \frac{C\hbar^2}{\mu}\frac{1}{z^3} + e\mathcal{F}\sin(\omega t + \gamma). \tag{31}$$

If we turn on the microwave field of frequency ω and amplitude $\mathcal{F}$ at time t_0, when the electron energy is $H_0(z, p, t_0) = -E_0$, a *measure* of the electron-energy change due to the interaction of the atom with the periodic electric field is given by

$$\varepsilon(t) := \frac{H_0\,(z(t),\, p(t),\, t)}{E_0}. \tag{32}$$

From the time-derivative of this equation and using Hamilton equations (31) we find that $\varepsilon(t)$ changes according to

$$\varepsilon(t) = -1 + \frac{e\mathcal{F}}{\mu E_0}\int_{t_0}^{t} {\rm d}t'\, p(t')\sin(\omega t' + \gamma). \tag{33}$$

In the limit $t \to \infty$, the integral of the right-hand side becomes the Fourier transformation of momentum $p(t)$. Therefore, the power spectrum of $p(t)$ could be used to distinguish periodic, quasiperiodic and chaotic motion [29].

For studying the ionization process we prepare the electron at an energy $-E_{0,n}$, and fix the field amplitude $\mathcal{F}$, the frequency ω and the phase γ. For each resonance ($n = 1, 2, 3, 4$) we characterize the different values of the electric-field amplitude $\mathcal{F}$ by a factor $r := \mathcal{F}/\mathcal{F}_n^{\rm cr}$,

where $\mathcal{F}_n^{\rm cr}$ is the Chirikov's critical electric-field amplitude obtained from (29) with $g = 1$ (see also table 2). Hereafter, we denote by $r_n^{\rm cr}$ the minimum value of r for which we have obtained ionization at the n-primary resonance.

We also introduce the scaled variables $Q = z/Q_0$, $P = p/P_0$, and $\tau = t/T_0$, where (Q_0, P_0, T_0) are free parameters. Thus, the image Hamiltonian $K(Q, P, t) = [T_0/(Q_0P_0)]\, H(QQ_0, PP_0, \tau T_0)$ leads to the Hamilton equations

$$\frac{{\rm d}Q}{{\rm d}\tau} = c_1 P \qquad \frac{{\rm d}P}{{\rm d}\tau} = -c_2\frac{(Z-\sigma)}{Q^2} + c_3\frac{C}{Q^3} + c_4\mathcal{F}\sin(\omega T_0\tau + \gamma) \tag{34}$$

with

$$c_1 := \frac{T_0P_0}{\mu Q_0} \qquad c_2 := \frac{T_0e^2}{Q_0^2P_0} \qquad c_3 := \frac{\hbar^2T_0}{\mu Q_0^3P_0} \qquad c_4 := \frac{T_0e}{P_0}.$$

Hydrogenic atoms ($\sigma = 0, C = 0$) obey classical scaling. Therefore, a standard selection is $Q_0 = n_0^2$, $P_0 = n_0^{-1}$ and $T_0 = n_0^3$. Here the dimensionless parameter n_0 is related to the initial classical principal action I_n and semi-classical quantization yields $I_n = \hbar n_0$ [1].

In the case of alkali atoms the potential energy $V_0(z)$ in (1) is a non-homogeneous function, hence $H_0(z, p)$ is not scalable. Then, for numerical calculation and plots we set (Q_0, P_0, T_0) in terms of characteristic properties of the unperturbed system (electric amplitude $\mathcal{F} = 0$), namely $Q_0 = z_1 - z_0$, $T_0 = T/2$ and $P_0 = \mu Q_0/T_0$.

We use the NDSolve package [30] with AccuracyGoal of 16, PrecisionGoal of 16 and WorkingPrecision of 24, to numerically solve the Hamilton equations (34) for the first four resonances of lithium and a microwave-field frequency $\omega = 1.509 \times 10^{-6}$ au.

4.1. Characterization and prediction of ionization for a single trajectory

In the *ionization* process the atom is excited by the interaction $V(t)$ to progressively higher energies and after a large enough time $t_{\rm I}$ ($t_{\rm I} > t_0$) the motion becomes unbounded. That is, for all time $t > t_{\rm I}$ the position grows indefinitely, and the momentum $p(t)$ and the energy $\varepsilon(t)$ become positive ($z(t) > 0$, $p(t) > 0$, $\varepsilon(t) > 0$). The *ionization time* of the system, along the trajectory under consideration, is the minimum value of $t_{\rm I}$ after which these conditions are permanently met. Since the electromagnetic field transfers energy to the electron, or takes energy from it, the energy $\varepsilon(t)$ can oscillate over a finite time interval, but if ionization has been achieved the sign of the energy must be positive for all $t > t_{\rm I}$.

Preparing the lithium atom with initial energy $-E_{0,1}$ corresponding to the *first primary resonance* ($n = 1$), we obtain ionization for electric-field amplitudes characterized by $r \geqslant 1$. Figure 1 illustrates the ionization process for $\mathcal{F} = \mathcal{F}_1^{\rm cr} = 6.08\,557 \times 10^{-10}$ au ($r = 1$) when the initial values of position and momentum correspond to the internal turning point and the initial phase of the microwave field is $\gamma = 5\pi/4$. Figures 1(*a*)–(*c*) show the time behaviour of $\varepsilon(\tau)$, $Q(\tau)$ and $P(\tau)$, respectively, while figure 1(*d*) depicts the points of the trajectory at regular time intervals given by $\Delta\tau = 10$ ($\Delta t = 10T_0$).

We observe in figures 1(*a*) and (*e*) that $\varepsilon(t)$ presents an energy-level jump structure which is more defined as the electron reaches higher energies. As expected, the jump actually occurs when the electron reaches the nearest distance to the core and collides with it (compare figures 1(*a*) and (*b*) for example at $\tau \cong 400$ and $\tau \cong 650$). Since the energy scale is different for each resonance, $E_0 = E_{0,n}$ in (32), the range values of ε at which this structure clearly appears are lower for higher resonances (see table 3). At high energies the movement of the electron between jumps follows a closed trajectory modulated by the field but when the final jump takes place the electron acquires enough energy to ionize and to follow an open trajectory.

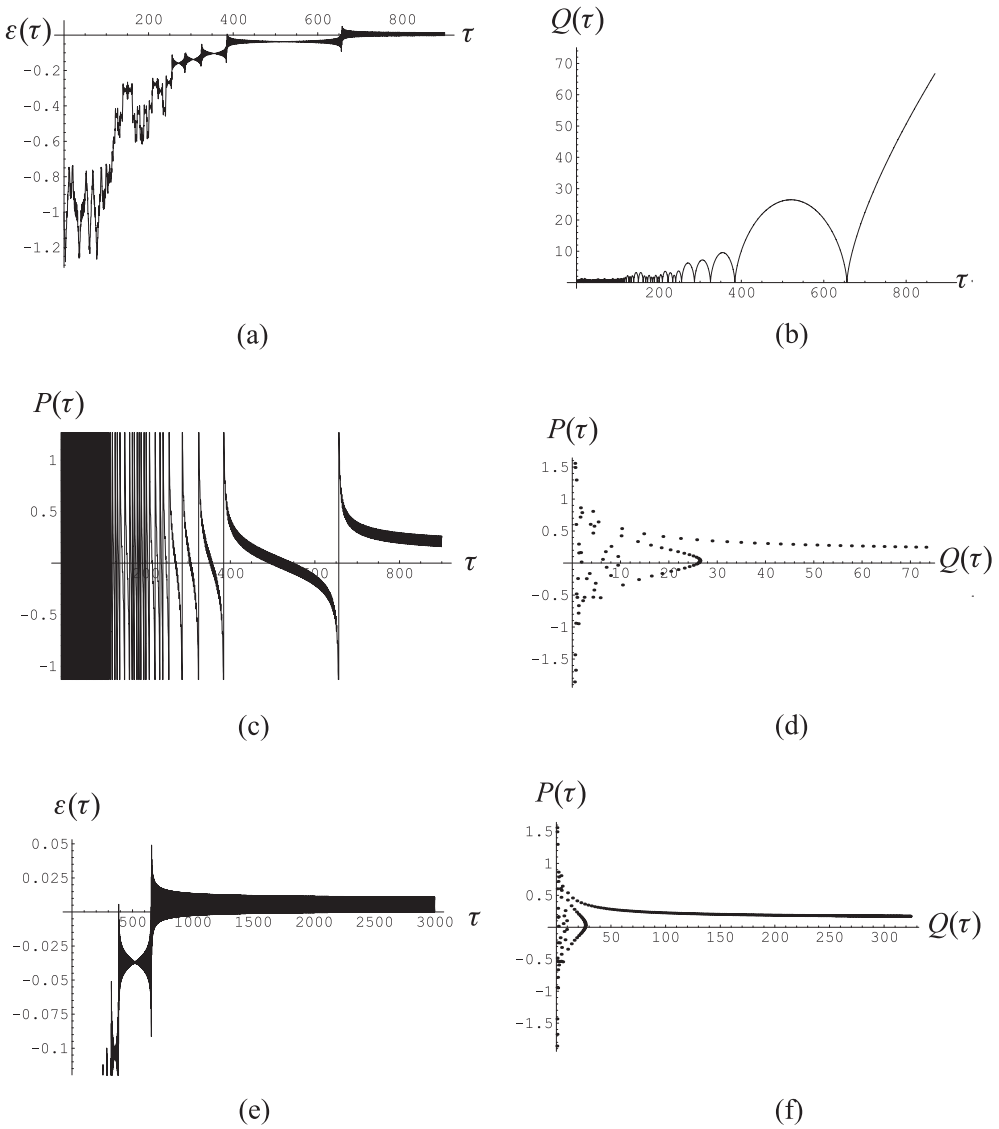

Figure 1. Lithium ionization at first primary resonance ($n = 1$) for microwave-field frequency $\omega = 1.509 \times 10^{-6}$ au, initial phase $\gamma = 5\pi/4$ and electric amplitude $\mathcal{F} = 6.085\,57 \times 10^{-10}$ au ($r_n^{\rm cr} = 1.0$): (*a*)–(*c*) show the time behaviour of $\varepsilon(\tau)$, $Q(\tau)$ and $P(\tau)$, respectively: (*d*) Depicts the phase-space trajectory: (*e*) and (*f*) show energy and trajectory behaviours for large times confirming the ionization process.

Since the electron absorbs energy from the field mainly when a jump occurs we can use this fact to *predict ionization* far before the ionization time $t_{\rm I}$ is reached for those cases when $\varepsilon(t)$ takes positive and negative values but oscillates near $\varepsilon = 0$. On this stage we define a time interval $t_a < t < t_b$ and evaluate the *time average of the energy*

$$\langle \varepsilon \rangle (t_a, t_b) := \frac{1}{t_b - t_a} \int_{t_a}^{t_b} \varepsilon(t')\, {\rm d}t' = \varepsilon(t_a) + \Delta\epsilon(t_a, t_b) \tag{35}$$

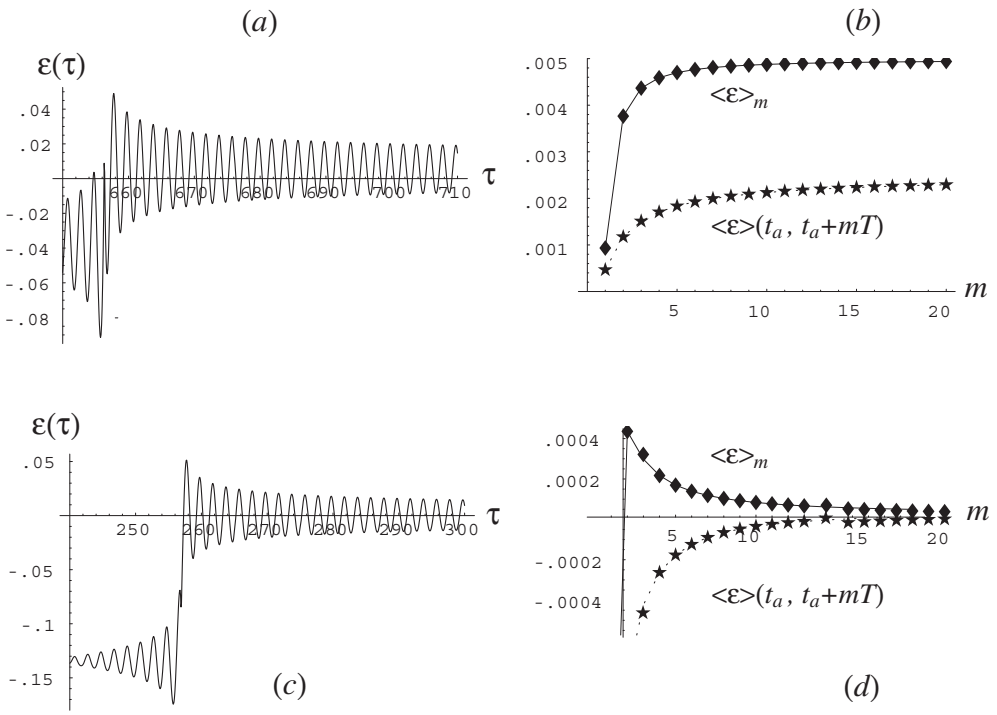

Figure 2. An electron's dynamical behaviour after the last jump in the case of the first resonance ($n = 1$), with the same initial conditions of figure 1 but different field phases: (a) $\gamma = 5\pi/4$, (c) $\gamma = (5\pi/4) + 0.06$. Figures (b) and (d) depict the behaviour of $\langle\varepsilon\rangle\,(t_a, t_a + mT)$ and $\langle\varepsilon\rangle_{\rm m}$ during the first 20 field cycles ($m = 1, 2, 3, \ldots, 20$) starting from t_a.

where the net change of energy between t_a and t_b is given by

$$\Delta\varepsilon(t_a, t_b) := \frac{e\mathcal{F}}{\mu E_0}\frac{1}{t_b - t_a}\int_{t_a}^{t_b} \mathrm{d}t'\,\big(t_b - t'\big)\,p(t')\sin\big(\omega t' + \gamma\big). \tag{36}$$

$\langle\varepsilon\rangle\,(t_a, t_b)$ gives the 'algebraic energy', counting energy as positive if $\varepsilon(t') > 0$ and as negative if $\varepsilon(t') < 0$. Since $t_b - t' > 0$, when $p(t') > 0$ the algebraic contributions to the integral (36) are determined exclusively by the function $\sin(\omega t' + \gamma)$.

Ionization prediction. Let t_a be the time at which the electron reaches the nearest distance to the core in the supposed last jump, $t_b = t_a + mT$, and $\langle\varepsilon\rangle_{\rm m} := \langle\varepsilon\rangle\,(t_a + (m-1)T, t_a + mT)$, where $T = 2\pi/\omega$ is the period of the field and m labels a set of time intervals ($m = 1, 2, 3, \ldots, M$). The atom will ionize if the classical trajectory of the active electron holds the following two properties: the time average of the energy in the interval $t_a < t < t_b$ is greater than zero ($\langle\varepsilon\rangle > 0$) for all $t_b > t_a$ and $\langle\varepsilon\rangle_{m+1} - \langle\varepsilon\rangle_{\rm m} > 0$ for all m. The last condition indicates that the electron is absorbing energy from the field and that for successive cycles the negative contributions of $\varepsilon(t)$ are decreasing.

Figure 2 illustrates the application of the above statement by comparing the ionization process of figure 1 with a non-ionization process. Figure 2(a) is a magnification of figure 1(a) after the last jump while figure 2(c) shows the behaviour of $\varepsilon(\tau)$ after the last jump for the same resonance ($n = 1$) but with a slightly different initial phase. The numerical calculations show that in case (c) there is no ionization before $\tau = 8000$, when the momentum has already taken

negative values. The corresponding behaviours of $\langle\varepsilon\rangle_{\rm m}$ and $\langle\varepsilon\rangle\,(t_a, t_a + mT)$ are depicted in figures 2(b) and (d). We recall that the electron absorbs energy from the field mainly during the first cycles. However, only in case (b), when the atom will ionize, it holds that $\langle\varepsilon\rangle_{m+1} - \langle\varepsilon\rangle_{\rm m} > 0$ and $\langle\varepsilon\rangle\,(t_a, t_a + mT) > 0$ for any $m = 1, 2, \ldots, 20$. That is, only in case (b) the absorbed energy from the field ($\Delta\varepsilon$ in equation (35)) is enough in order for $\langle\varepsilon\rangle\,(t_a, t)$ to become positive for $t > t_a$.

The above property is useful since we can predict ionization by analysing the energy behaviour in the time interval $t_a < t < t_b$, far before the ionization time $t_{\rm I}$. In this way we can avoid long calculations by ending them at $t_b \ll t_{\rm I}$. For example, in figures 1(a) and (c) we find $\tau_a \cong 656$ ($t_a \cong 656T_0$) but the figure 1(e) shows that the ionization time could be around $t_{\rm I} \cong 2300T_0$. The last figure includes calculations in the interval $\tau \in [0, 3000]$ in order to confirm the fulfilment of the ionization conditions.

In the case of *second, third and fourth resonances* ($n = 2, 3, 4$) we observe similar general behaviour to that obtained for $n = 1$. With the precision and accuracy already quoted, and the initial phases $\gamma = 5\pi/4$ and $3\pi/2$, and $\tau <\approx 3000$, we find the following critical values: $r_1^{\rm cr} = 1.0 \pm \Delta r$, $r_2^{\rm cr} = 1.1 \pm \Delta r$, $r_3^{\rm cr} = 1.2 \pm \Delta r$, and $r_4^{\rm cr} = 1.4 \pm \Delta r$ ($\Delta r = 0.05$). In all cases $r_n^{\rm cr} \geqslant 1$ and this value increases with n. That is, ionization at Chirikov's critical electric amplitude $\mathcal{F}_n^{\rm cr}$ with $g = 1$ is obtained only for the first resonance. Clearly the two-thirds heuristic rule does not improve in our case the prediction of the critical electric fields. Figures 3(a)–(d) show the behaviour of the ionization process for the electric-field amplitudes corresponding to these $r_n^{\rm cr}$ critical values ($n = 1, 2, 3, 4$).

4.2. The role of the microwave-field γ phase

We observe a strong dependence between the dynamical behaviour of the electron and the value of the field's phase γ. As an example, figure 4 shows that the initial behaviour of $\epsilon(\tau)$ and the ionization time $\tau_{\rm I}$ depend on the value of γ. In all the cases shown in this figure ($\gamma = 3\pi/2, 5\pi/4, \pi, 3\pi/4, \pi/2, \pi/4$), the field is turned on at $\tau_0 = 0$, the initial energy of the electron is $-E_{0,1}$, the electric-field amplitude corresponds to $r = 5$, and the initial position and momentum are $Q(0) = z_0$, $P(0) = 0$.

However, the corresponding trajectories are not physically equivalent. Actually, for some values of γ ($5\pi/4, \pi, \pi/4$) there are ionization while for other values of γ ($3\pi/2, 3\pi/4, \pi/2$) the electron remains bounded. As we show below, the variation of γ is physically equivalent to change the initial surface energy, below or above $-E_{0,1}$. This change increases with the intensity of the applied microwave field.

The phase dependence of the ionization can be understood by applying to (34) the time transformation $\tilde{\tau} := \tau + \tau_\gamma$, with $\tau_\gamma := \gamma/(\omega T_0)$, and introducing the new dependent variables, $\tilde{Q}(\tilde{\tau}) := Q\left(\tilde{\tau} - \tau_\gamma\right)$ and $\tilde{P}(\tilde{\tau}) := P\left(\tilde{\tau} - \tau_\gamma\right)$. The resulting equations of motion for $(\tilde{Q}(\tilde{\tau}), \tilde{P}(\tilde{\tau}))$ become independent of the parameter γ; hereafter they will be referred as $(34)_{\gamma=0}$. Since the initial conditions are fixed at the times $\tilde{\tau}_0$ and τ_0, respectively, and $\tilde{\tau}_0 := \tau_0 + \tau_\gamma$, the set of equations $(34)_{\gamma=0}$ is *physically equivalent* to the original one (34) if the initial conditions are connected by $\tilde{Q}(\tilde{\tau}_0) = Q(\tau_0)$ and $\tilde{P}(\tilde{\tau}_0) = P(\tau_0)$. For example, $\tilde{Q}(\tau_\gamma) = Q(0)$ and $\tilde{P}(\tau_\gamma) = P(0)$ or $\tilde{Q}(0) = Q(-\tau_\gamma)$ and $\tilde{P}(0) = P(-\tau_\gamma)$.

As a consequence of the above considerations we conclude that the trajectories $(Q(\tau), P(\tau))_\gamma$, which correspond to the calculations of $\varepsilon(\tau)$ shown in figure 4 for several values of γ, are not physically equivalent to each other. In fact, the phase γ induces changes on the dynamical behaviour of the electron and depending on the value of γ the active electron remains bounded or ionizes.

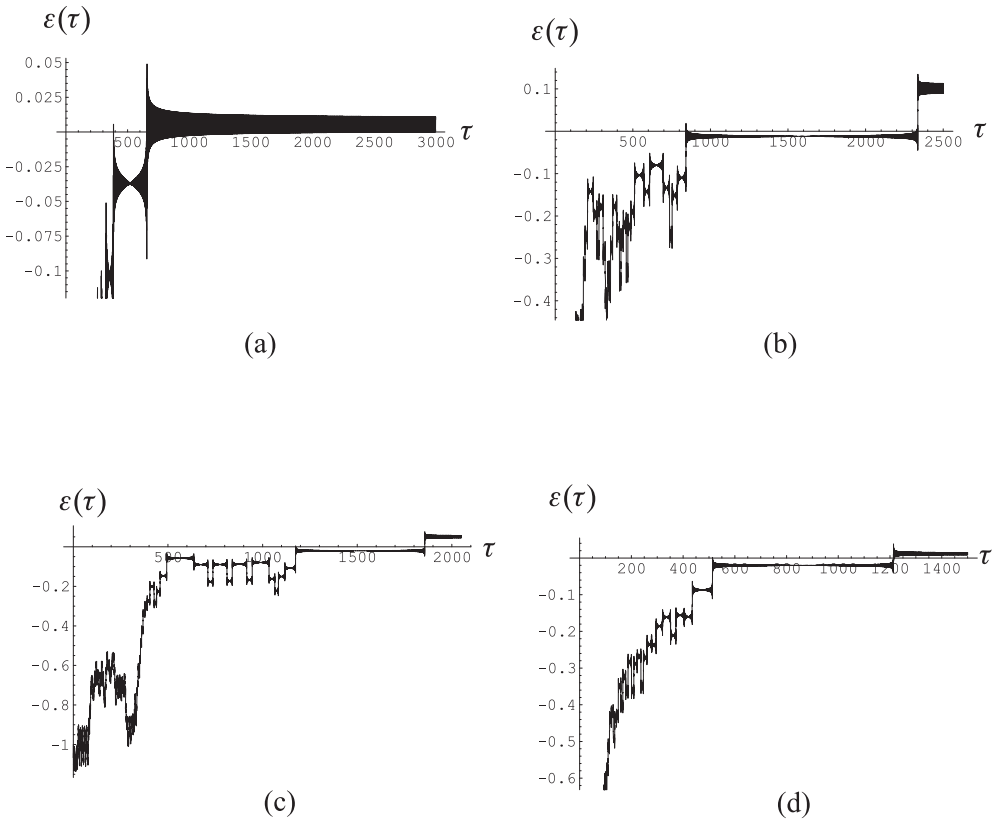

Figure 3. Lithium ionization at (*a*) first, (*b*) second, (*c*) third and (*d*) fourth primary resonances with microwave-field frequency $\omega = 1.509 \times 10^{-6}$ au and electric-field amplitudes corresponding to critical values $r_1^{\rm cr} = 1.0$ ($\mathcal{F} = 6.085\,57 \times 10^{-10}$ au), $r_2^{\rm cr} = 1.1$ ($\mathcal{F} = 2.5892 \times 10^{-10}$ au), $r_3^{\rm cr} = 1.2$ ($\mathcal{F} = 1.552\,97 \times 10^{-10}$ au) and $r_4^{\rm cr} = 1.4$ ($\mathcal{F} = 1.167\,88 \times 10^{-10}$ au). The microwave field's phase γ is: for (*a*), (*c*) and (*d*), $\gamma = 5\pi/4$, and for (*b*), $\gamma = 3\pi/2$.

Note that in order to obtain physically equivalent trajectories with different values of γ there is at least two possible procedures. The first one requires one to start the integration of $(34)_{\gamma=0}$ at the initial time $\tilde{\tau}_0 = \tau_\gamma$, instead of $\tilde{\tau}_0 = 0$, and fix $(Q(0), P(0))$ as the initial phase-space point of the trajectory. In this case the initial energy of the electron is the energy $-E_{0,n}$ of the nth primary resonance ($n = 1$ in the case of figure 4).

In the second procedure we choose as the starting point of $(34)_{\gamma=0}$ the time $\tilde{\tau}_0 = 0$. However, the initial condition $(\tilde{Q}(0), \tilde{P}(0))$ must be initially determined by time evolution of the point $(Q(0), P(0))$ backwards to the time $-\tau_\gamma$. This is done using (34) that describes the full perturbed alkali atom in the microwave field with phase γ. As a consequence of this backward time evolution the energy of the active electron changes and, therefore, the initial energy for $(34)_{\gamma=0}$ at initial time $\tilde{\tau}_0 = 0$ is different to the nth primary resonance energy $-E_{0,n}$.

As an example, figure 5 shows the points $(Q(-\tau_\gamma), P(-\tau_\gamma))_\gamma$ at which the trajectories have to be launched at $\tilde{\tau}_0 = 0$ in order to obtain physically equivalent trajectories for the values of γ considered in figure 4. For $\gamma = 3\pi/2$ the point lies below the first resonance, for $5\pi/4$ and $\pi/4$ the points are near before and near after the first resonance but above the second resonance, and for π, $3\pi/4$ and $\pi/2$ the points are above the second resonance.

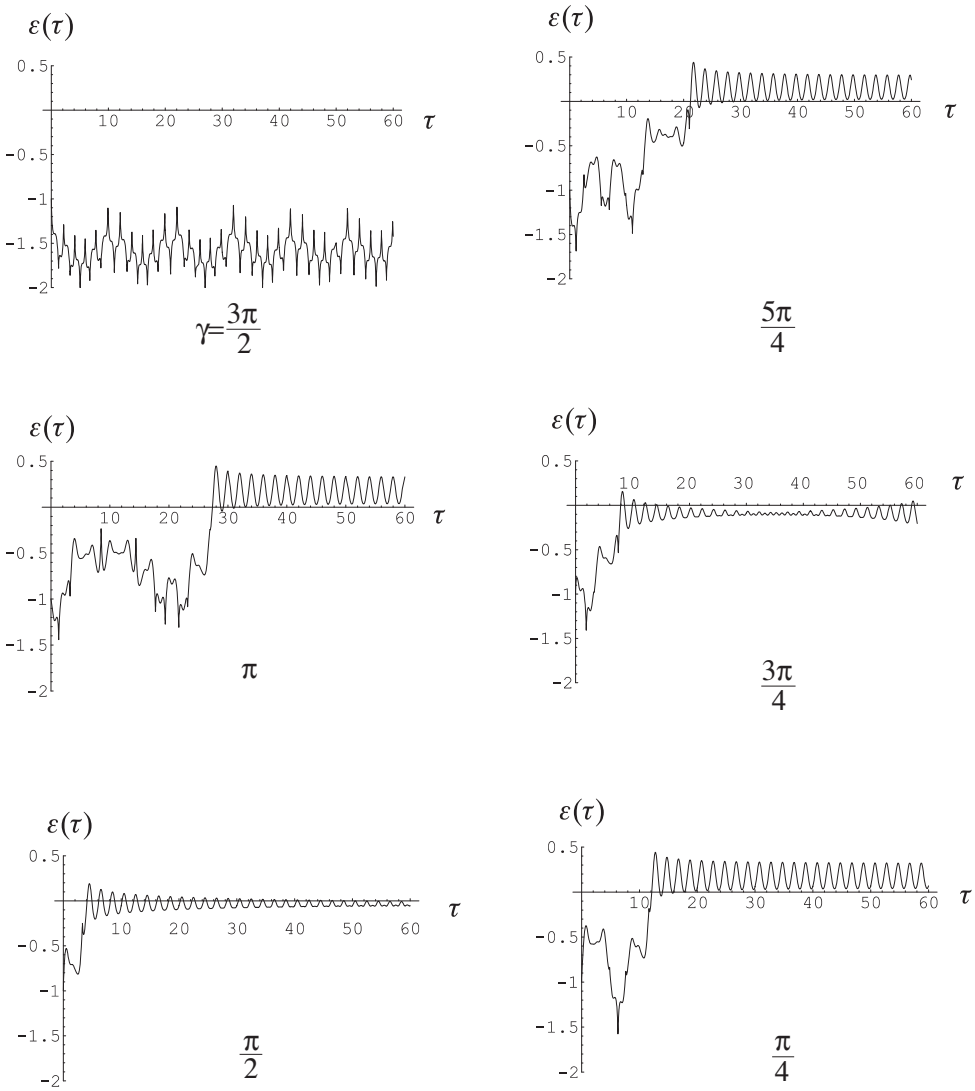

Figure 4. Dynamical dependence of $\varepsilon(\tau)$ with microwave field's phase γ for the first resonance ($n = 1$), microwave-field frequency $\omega = 1.509 \times 10^{-6}$ au and electric-field amplitude $\mathcal{F} = 3.042\,78 \times 10^{-9}$ au ($r = 5.0$). The values of γ are specified in the figures.

Note in figure 5 that in some of these cases ($\gamma = \pi, 3\pi/4, \pi/2$) the new initial energy is now in the neighbourhood of the second primary resonance ($-E_{0,2}$) instead of the first one ($-E_{0,1}$).

In conclusion, in the first procedure the effect of γ is equivalent to the standard interpretation of turning on the field at a time τ_γ while the electron remains at the same phase space point of the chosen resonant energy surface $-E_{0,n}$. The second procedure is equivalent to turning on the field at $\tau_0 = 0$ but the electron must be initially localized on a higher or lower energy surface than the resonant one, $-E_{0,n}$. In this case the position of the point depends on the field intensity and the phase γ. We point out that, in accordance with the second interpretation, the values of γ used for figure 3 assure that the electron is initially in the vicinity of the unperturbed resonant energy surface $-E_{0,n}$, with $n = 1, 2, 3, 4$.

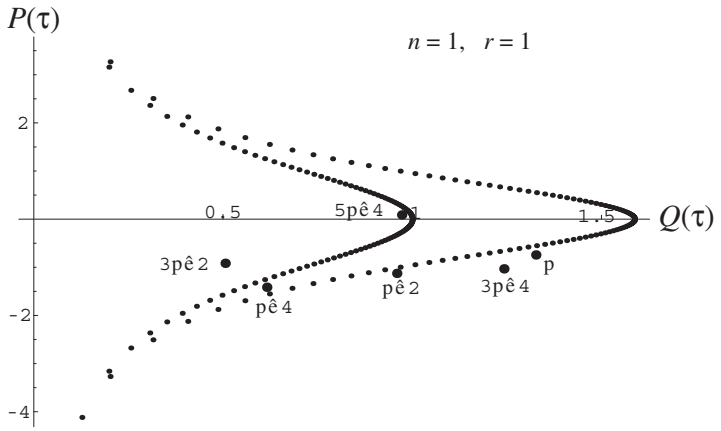

Figure 5. Initial phase-space points determined by backward time evolution from $(Q(0), P(0))$ to $(Q(-\tau_\gamma), P(-\tau_\gamma))$ for the different values of γ considered in figure 4. These initial conditions, the initial time $\tilde{\tau}_0 = 0$, and (34) at $\gamma = 0$ allow one to calculate physically equivalent trajectories corresponding to the cases treated in figure 4 ($n = 1, r = 5$). The background curves are phase-space trajectories for the unperturbed atom at energies of $-E_{0,1}$ and $-E_{0,2}$.

To end this section we present in figure 6 the structure of the phase space for the first resonance ($n = 1$), at Chirikov's critical field $r = 1$ and for the values of γ considered in figure 2 ($5\pi/4, 5\pi/4 + 0.06$). The Poincaré surface of sections in action-angle variables, $\theta(mT) - I(mT)$, are generated with approximately 100 trajectories and each trajectory contributes with 400 *thin* points ($m = 1, 2, \ldots, 400$); T is the period of the field. For both values of γ the global structure of the phase space looks alike, but there is a small shift in the angle variable θ, a weak distortion of the tori and some resonances are more notorious for the case of $\gamma = 5\pi/4 + 0.06$.

We superpose to each Poincaré section a set of *thick* points which are generated by the contribution of the same single trajectory considered in figure 2, with initial condition $(z_0, 0)$ and first-resonance energy $E_0 = 7.473\,526\,7435\,10^{-5}$ au. When m augments the representative point jumps from here to there, up and down.

The main effect of changing γ is a modification in the behaviour of the embedded trajectory. For $\gamma = 5\pi/4 + 0.06$ the representative point visits the region in the vicinity of the first resonance more frequently and, therefore, generates nearby it a high density of thick points. When $\gamma = 5\pi/4$ the visited region in the neighbourhood of the first resonance is wider and the density of the thick points is lower. In this case, when m augments, the action $I(mT)$ progressively has a net increase and the trajectory finally ionizes at a time t_I far beyond the 400 periods used for doing the Poincaré surface of the section (see figures 1 and 2). In the other case ($\gamma = 5\pi/4 + 0.06$) the calculations show that there is no ionization.

5. Conclusions

We have successfully applied a simple one-dimensional model to study the classical dynamics of alkali atoms under microwave fields, which allows an explicit visualization of the classical ionization process induced by chaos. Regular or chaotic motion of the valence electron is observed depending on the values of the perturbation parameters, namely, frequency and electric-amplitude of the microwave field.

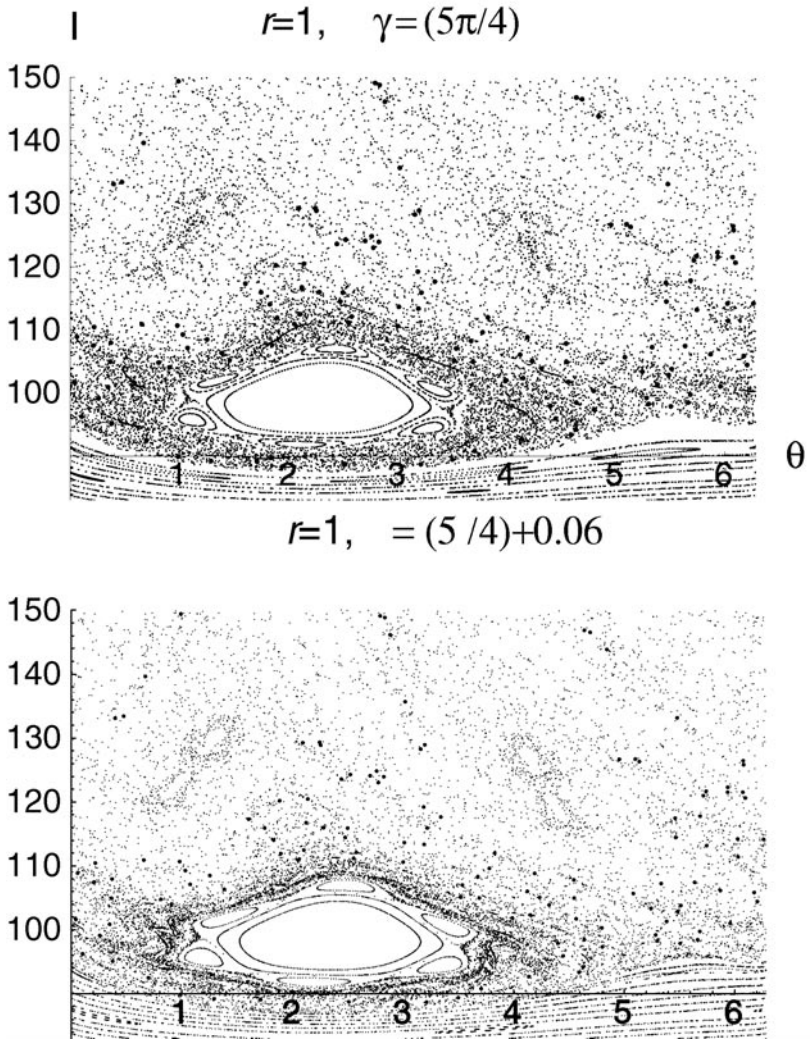

Figure 6. Poincaré surface of sections for the two values of γ considered in figure 2 which correspond to an ionization case ($\gamma = 5\pi/4$) and a non-ionization process ($\gamma = 5\pi/4 + 0.06$). In each figure, the *thick* points represent the contribution of a single trajectory with initial condition $(z_0, 0)$ and first-resonance energy, which has been superposed onto the Poincaré section surface (*thin* points).

We have used Chirikov's overlap criterion to estimate the critical electric-field amplitude at which ionization occurs and have tested this prediction by integration of Hamilton equations. The obtained numerical values for the critical electric field-amplitude validate the order of magnitude of Chirikov's predictions for low resonances and show that Chirikov's original approach ($g = 1$) is, in this case, superior to the two-thirds heuristic rule.

We have shown that ionization dynamics for a single trajectory depends on the γ phase. The results show that by changing γ we can obtain physically equivalent trajectories if the field is turned on at $\tau = 0$ and the electron is initially localized on a suitable energy surface different to the resonant one, $-E_{0,n}$.

In some cases, depending on the system's parameters, the ionization time t_I is too large and in principle a large amount of computational effort is required. Similarly, when $\varepsilon(t)$ is oscillating near over $\varepsilon = 0$ but the trajectory does not ionize, the electron remains trapped by the core potential during a thousand field cycles on a very long closed trajectory. For both cases and by using some basic ideas we developed a method for predicting ionization far before the time t_I is reached. This is a very useful technique that avoids long calculations involving the numerical integration of Hamilton equations.

Let us conclude this section with some comparisons between hydrogen-like atoms and alkali atoms. The Hamiltonian (2) with $C \neq 0$ is not invariant with respect to scaling transformations, unlike (2) for hydrogenic atoms ($C = 0, \sigma = 0$). Thus, the ionization-threshold when $C \neq 0$ depends on three independent variables $(E_0, \omega, \mathcal{F})$. In the case of hydrogenic atoms, to the contrary, the ionization threshold depends on two scaled variables: the scaled frequency $\tilde{\omega} := n_o^3\,\omega$ and the scaled amplitude $\tilde{\mathcal{F}} := n_o^4\,\mathcal{F}$.

A final noteworthy difference between hydrogenic and alkali atoms is that the former parameter z_0 in (3) vanishes causing a singularity at $z = 0$ in Hamilton's motion equations (31). To avoid this singularity special variables or procedures are needed to deal with it. In the case of alkali atoms $C > 0$, the turning point z_0 is positive and the inequality $z_0 > 0$ defines a singularity-free motion region.

Acknowledgments

One of the authors (JM) received important support from the 'Fundación Mazda para el Arte y la Ciencia', Bogotá. Fruitful discussions with J D Urbina, C Viviescas and T Dittrich are gratefully acknowledged. The authors are grateful to one of the referees for helpful remarks. This work was partially supported by DINAIN of the 'Universidad Nacional de Colombia' under the project Complex Dynamics of Nonlinear Systems, and by COLCIENCIAS.

References

[1] Koch P M 1992 Atomic and molecular physics experiments in quantum chaology *Chaos and Quantum Chaos* ed W D Heiss (Berlin: Springer) pp 167–224
[2] Leopold J G and Percival L C 1978 *Phys. Rev. Lett.* **41** 944
[3] Bayfield J E and Koch P M 1974 *Phys. Rev. Lett.* **33** 258
[4] Koch P M and van Leeuwen K A H 1995 *Phys. Rep.* **255** 289
[5] Casati G, Chirikov B V, Shepelyansky D L and Guarneri I 1987 *Phys. Rep.* **154** 77
[6] Jensen R V, Susskind S M and Sanders M M 1991 *Phys. Rep.* **201** 1
[7] Blümel R and Reinhart W P 1997 *Chaos in Atomic Physics* (Cambridge: Cambridge University Press)
[8] Richards D 1997 The periodically driven exited hydrogen atom *Lectures Notes in Physics: Classical, Semiclassical and Quantum Dynamics in Atoms* vol 485, ed H Friedrich and B Eckhardt (Berlin: Springer) pp 173–204
[9] Galvez E J, Sauer B E, Moorman L, Koch P M and Richards D 1988 *Phys. Rev. Lett.* **61** 2011
[10] Bayfield J E, Casati G, Guarneri I and Sokol D W 1989 *Phys. Rev. Lett.* **63** 364
[11] Gallagher T F, Mahon C R, Pillet P, Fu P and Newman J B 1989 *Phys. Rev.* A **39** 4545
[12] Panming Fu, Scholz T J, Hettema J M and Gallagher T F 1990 *Phys. Rev. Lett.* **64** 511
[13] Benson O, Buchleitner A, Raithel G, Arndt M, Mantegna R N and Walther H 1995 *Phys. Rev.* A **51** 4862
[14] Buchleitner A, Delande D, Zakrzewski J, Mantegna R N, Arndt M and Walther H 1995 *Phys. Rev. Lett.* **75** 3818
[15] Krug A and Buchleitner A 2000 *Europhys. Lett.* **49** 176
[16] Eder G 1968 *Quantenmechanik I* (Mannheim: Bibliographisches Institut)
[17] Burns M and Reichl L E 1992 *Phys. Rev.* A **45** 333
[18] Friedrich H 1991 *Theoretical Atomic Physics* (Berlin: Springer)
[19] Leopold J G and Richards D 1991 *J. Phys. B: At. Mol. Opt. Phys.* **24** 1209
[20] Chirikov B V 1979 *Phys. Rep.* **52** 263–379

[21] Jensen R V 1984 *Phys. Rev.* A **30** 386
[22] Lichtenberg A J and Lieberman M A 1992 *Regular and Chaotic Dynamics* (Berlin: Springer)
[23] Schwartz L 1966 *Mathematics for the Physical Sciences* (Reading, MA: Addison-Wesley)
[24] Relton F E 1965 *Applied Bessel Functions* (New York: Dover)
[25] Copson E T 1967 *Asymptotic Expansions* (Cambridge: Cambridge University Press)
[26] Sirovich L 1971 *Tecniques of Asymptotic Analysis* (New York: Springer)
[27] Sacha K and Zakrzewski 1997 *Phys. Rev.* A **55** 568
[28] Sacha K and Zakrzewski 1997 *Phys. Rev.* A **56** 719
[29] Tufillaro N B 1992 *An Experimental Approach to Nonlinear Dynamics and Chaos* 3rd edn (Redwood City: Addison-Wesley)
[30] Wolfram S 1996 *The Mathematica Book* 3rd edn (Cambridge: Cambridge University Press)